

## INTERMEDIATE BALLISTICS UNSTEADY SABOT SEPARATION: FIRST COMPUTATIONS AND VALIDATIONS

**Dr. R. Cayzac<sup>1</sup>, Mr. E. Carette<sup>1</sup> and Pr. T. Alziary de Roquefort<sup>2</sup>**

<sup>1</sup> *Giat Industries, Division des Systèmes d'Armes et de Munitions, 7 Route de Guerry, 18023 Bourges Cedex, France*

<sup>2</sup> *Université de Poitiers, Laboratoire d'Etudes Aérodynamiques, 43 Rue de l'Aérodrome, 86036 Poitiers Cedex, France*

A first and recent attempt, based on the 2D Euler equations, has been carried out at the unsteady numerical prediction of the sabot separation process in intermediate ballistic flow conditions. For validation purposes, the 44 mm APFSDS launch dynamics were investigated in a free flight ballistic corridor. Experimental test cases of drag, lift and rear separation processes were obtained. Comparisons between experimental and numerical sabot separation show satisfactory agreement.

## INTRODUCTION

### Challenge

The numerical unsteady prediction of the sabot discard in intermediate ballistic flow conditions is a challenge for the future. To date, highly sophisticated but purely external aerodynamics with a steady CFD approaches have been carried out [1–5]. A first attempt at unsteady prediction was made by extending the FREIN [6–12] intermediate ballistics code. The idea is to anticipate the main numerical problems of the modeling by using simple theoretical assumptions (Euler equations, 2D, . . .) as a first step.

### Separation Processes: A Non Exhaustive Classification

Figure 1 is a diagram of the possible discard processes.

Drag separation could be obtained using a classical external sabot profile with a front pocket. Separation is essentially the sudden rotation of the sabot components, a contact being made between the projectile body and the rear part of the sabot components. In this case, the mechanical interactions are substantial. Drag separation is obtained by “pitch moment”.

The lift separation process could be produced by the presence of a rear or middle pocket. The intermediate ballistic flow is employed. During the first instants, discard is

guided by the gas discharge with a rear separation. After that, separation is characterized by a quasi-parallel escape between the firing axis and the longitudinal axis of the sabot components. In this case, the mechanical interactions are fewer. Lift separation could be reached by “force” or by “moment”.

Rear separation, in the initial opening stage, could be obtained using a sabot with a rear pocket and with, or without, a front pocket of reduced efficiency.

## EXPERIMENTAL SET-UP AND TEST CONDITIONS

### Apparatus and Instrumentation

Figure 2 is a diagram of the experimental set-up for the tests. They were conducted in the 200 m free flight ballistics corridor at Giat Industries in Bourges. A 44 mm smooth-bore gun with a 4.53 m barrel and a specific APFSDS projectile, launched by a sabot with 3 components, were used for the tests. The projectile had a length to diameter ratio (L/D) of 23.75, a total mass of 0.475 kg including a sabot mass of about 0.2 kg and was identical for all tests. The intermediate ballistics of the projectile (sabot discard and muzzle blast characteristics) were investigated by use of a multiple orthogonal X-Ray technique (1 station at the muzzle and 3 orthogonal stations, located at 0.00, 0.15, 0.60 and 1.60 meters from the muzzle exit), by visualization of the muzzle flow field by indirect shadow system with Fresnel-Lens and also by ground pressure measurements.

### Test Conditions and Sabot Design

With 0.42 kg of a single base nitrocellulose propellant, the pressure chamber was of 252 MPa, the muzzle exit velocity was about 1443 m/s with a muzzle pressure of about 21 MPa.

Three different sabot shapes (versions ①, ② and ③), with or without a rear pocket, were tested and are presented in Fig. 3. Version ① is a classical shape with a front pocket. Version ② is characterized by a rear pocket, the front pocket being suppressed. Version ③ is a compromise having a rear pocket and a reduced front pocket. For all the versions, the position of the center of gravity, the mass and the inertia, the length of the body-sabot interface, the sealing ring definition and behavior, the guiding support definitions, the interface and the mechanical contacts between the sabot components remain as constant as possible. Note that the mass of the powder was adapted in order to prevent the sabot pocket from breaking. The mechanical performance of the sabot was verified using structural computations taking into account only the longitudinal acceleration. The sabot profile (rear pocket, ...) was designed essentially empirically.

More than 50 firings were carried out for version ①, 3 for versions ② and ③.

## CFD, Equations and Numerical Algorithms

An intermediate ballistic code, named FREIN, based on the resolution of the time dependent 2D Euler equations, has been developed. The FREIN code has now been extended to the modeling of the unsteady sabot separation in intermediate ballistic flow conditions.

The discharge of a propellant gas is modeled as an axisymmetric or 2D plan inviscid flow of a calorically perfect gas and is computed using Harten's 2<sup>nd</sup> order total variation diminishing scheme. The complex geometry, evolving over time because of the displacement of the projectile, is taken into account, within the framework of a non adapted uniform Cartesian mesh, by means of a special treatment of the boundary conditions based on a generalized reflection principle. The gas behaves as a calorically perfect gas, the ratio of specific heats  $\gamma$  and the perfect gas constant  $R$  of the equation of state  $p = \gamma RT$  were obtained using thermodynamic computations. Moreover, the ambient atmosphere was not distinguished from the propellant gas.

The mathematical modeling of the firing process includes the precursor flow discharge and the presence of the projectile. The boundary conditions at the barrel muzzle, after projectile exit, were computed using a 1D unsteady numerical code, based on the characteristics method, according to a pull piston analogy. The boundary conditions at the barrel muzzle, before the projectile exit, were obtained with the resolution of the 1D Euler equations according to a push piston analogy.

The sabot component trajectory was computed using calculations of the unsteady aerodynamic forces and of the actions of contact.

The main difficulties related to the grid system are firstly, the rather complex geometry involved (in particular in the multi-elements muzzle brake case) and secondly, the fact that the computational domain evolves over time according to the displacement of the projectile and the sabot.

## CFD, Grid and Calculation Costs

For the 3 versions of sabot, the computational domain is 2.5 m x 0.3 m. The Cartesian grid is constituted of 270 000 nodes with a spatial step size  $\Delta x = \Delta y$  of about 1.67 mm. In the case of the lift sabot opening (version ③) a more refined grid was also built with 1 080 000 nodes and  $\Delta x = \Delta y$  of about 0.83 mm (see results in Fig. 8).

The average calculation cost is about 2.1  $\mu$ s per node and per iteration, for unsteady computations on an Octane SGI RISC 12000 workstation.

## RESULTS

### CFD: Intermediate Ballistics Flow Field Analysis

Figure 4 gives an example of the time history of the intermediate ballistic flow corresponding to the drag separation process (version ①). The precursor flow and the principal

propellant gas flow are highlighted. The main structures of the unsteady overexpanded jet flow (Mach disk, barrel shock and blast wave), of the projectile and sabot aerodynamics, are numerically well captured. In particular, we can see:

- the strong interaction between the projectile-sabot and the Mach disk ( $t = 3.5$  ms),
- the interaction between the projectile nose and the blast wave ( $4.1 \leq t \leq 4.9$  ms),
- the mechanical and aerodynamic sabot-projectile interactions of the drag discard ( $3.7 \leq t \leq 4.9$  ms).

## Experiments: Sabot Discard Processes (X-Ray Visualizations)

Figures 5, 6 and 7 show that the different separation processes have been obtained.

Version ① is characterized by drag separation. At 0.6 m from the muzzle, the sabot components are parallel to the projectile with a gap of approximately 4 mm. Taking into account the fact that, for this sabot shape, it is the gas discharge which holds the sabot components locked together, this gap could be explained by the relaxation of the internal ballistic constraints of the sabot components. At 1.6 m, the drag separation process is visualized. A rear contact between the projectile body and the sabot components shows the mechanical interactions. Version ② is characterized by rear separation due to the gas flow discharge. As shown in Fig. 7, lift separation was obtained with version ③. At 0.6 m from the muzzle, there is slight rear separation. At 1.6 m, the sabot components are parallel to the projectile and the mechanical interactions are minimal.

The X-Ray visualizations presented confirm the possibility of being able to pilot the separation by making judicious use of the intermediate ballistic flow.

## Validation: Prediction of the Separation Process

Qualitative validation results for the prediction of the different separation processes are presented in Figs. 5, 6 and 7. Fairly good agreement was obtained for the prediction of drag (Fig. 5, version ①) and on the rear discard processes (Fig. 6, version ②). Steady computations are in poor agreement with experiments in the case of the lift separation process (Fig. 7 C et D, version ③). The main reasons for this are the actual modeling limitations for such unsteady flow and also the specific weakness of the lift force. A complementary analysis is under way. Firstly the influence of the grid refinement was evaluated. The comparison between Fig. 7 and Fig. 8 shows, classically, that grid refinement has a strong influence on the numerical capture of the flow characteristics, but only slight changes to the opening kinematics could be observed.

## CONCLUSIONS

For validation purposes, drag, rear and lift separations were successfully obtained experimentally for a 44 mm gun using different sabot shapes. Numerical Euler techniques have been successfully developed for the prediction of the unsteady sabot separation pro-

cess. Qualitative validation results are globally encouraging, but the short comings of the 2D Euler equations are highlighted.

## FURTHER INVESTIGATIONS

With the French State support, further investigations are planned, principally:

- to fully analyze the limit of the 2D Euler equations,
- to extend the capability of the FREIN code to 3D,
- to develop more detailed small-scale intermediate ballistic experiments.

## REFERENCES

1. F. Lesage and M.J. Raw, "Navier-Stokes Computation of the Aerodynamics of Symmetric Sabot Separation", *13<sup>th</sup> International Symposium on Ballistics*, Stockholm, Sweden, (1992).
2. L. Yean-Kai, T. Chang-Hsien, H. Wen-Hu and L.M. Fulong, "High-Resolution Navier-Stokes Computations of a Sabot Separating from a Gun-Lunched Projectile with Turbulence Model", *14<sup>th</sup> International Symposium on Ballistics*, Quebec, Canada, (1993).
3. E.N. Ferry, J. Sahu and K.R. Heavy, "Navier-Stokes Computation of Sabot Discard Using Chimera Scheme", *16<sup>th</sup> International Symposium on Ballistics*, San Francisco, USA, (1996).
4. P. Champigny, P. d'Espiney and D. Ceroni, "Computation of Sabot Discard Using Chimera Technique", *17<sup>th</sup> International Symposium on Ballistics*, Midrand, South Africa, (1998).
5. A. Mikhail and K. Heavy, "Sabot Opening Lift Force: Analysis, CFD, and Test", *38<sup>th</sup> Aerospace Sciences Meeting & Exhibit*, Reno, USA, (2000).
6. T. Alziary de Roquefort, R. Cayzac, E. Carette and P. Balbo, "Theoretical and Experimental Comparison of Unsteady Flow Through a Muzzle Brake", *13<sup>th</sup> International Symposium on Ballistics*, Stockholm, Sweden, (1992).
7. R. Cayzac, A. Mennechet and E. Carette, "Sources of Dispersion Occurring with APFSDS Launch Dynamics", *15<sup>th</sup> International Symposium on Ballistics*, Jerusalem, Israel, (1995).
8. R. Cayzac, C. Vaglio, J. Brossard, E. Carette and T. Alziary de Roquefort, "Transitional Ballistic Investigations", *47<sup>th</sup> Aeroballistic Range Association Meeting*, ISL, Saint-Louis, France, (1996).
9. R. Cayzac, C. Vaglio, J. Brossard, E. Carette and T. Alziary de Roquefort, "Intermediate Ballistic Computations and Comparison with Firing Tests", *17<sup>th</sup> International Symposium on Ballistics*, Midrand, South Africa, (1998).
10. D. Boisson, R. Cayzac and G. Legeret, "Study of the Heat Exchanges Occuring During the Cooling Phase in a Gun Barrel", *18<sup>th</sup> International Symposium on Ballistics*, San Antonio, USA, (1999).
11. D. Boisson, R. Cayzac and G. Legeret, "Study of the Gas Discharge and the Heat Exchanges Occuring in a Gun Barrel After the Projectile Leaves the Barrel – Validation for the 30 mm Gun", *European Forum on Ballistics of Projectiles*, ISL, Saint Louis, France, (2000).
12. R. Cayzac and E. Carette, "Intermediate Ballistics and Aeroballistics Overview", *European Forum on Ballistics of Projectiles*, ISL, Saint Louis, France, (2000).

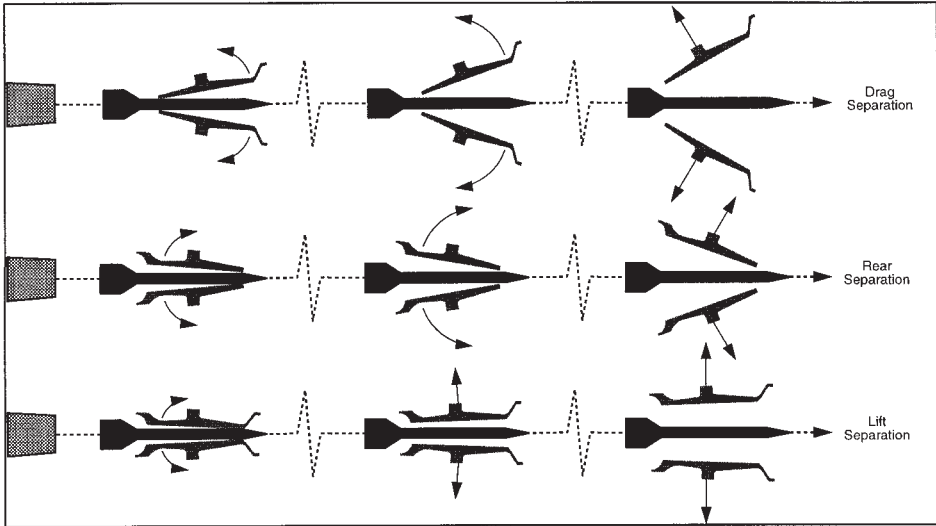


Fig. 1: Diagram of possible discard processes.

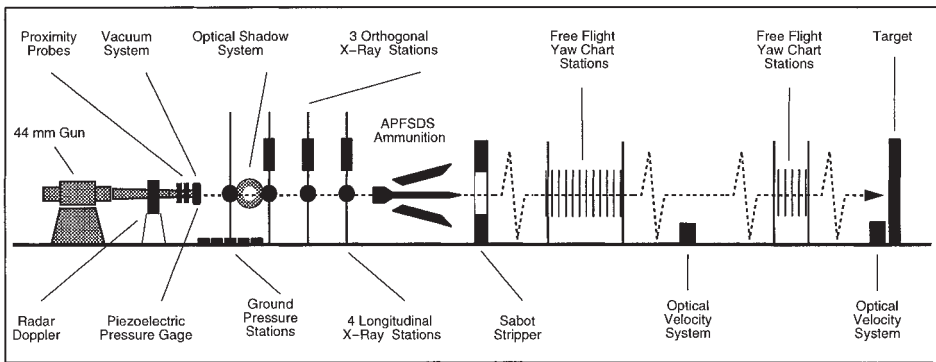


Fig. 2: Diagram of the test set-up.

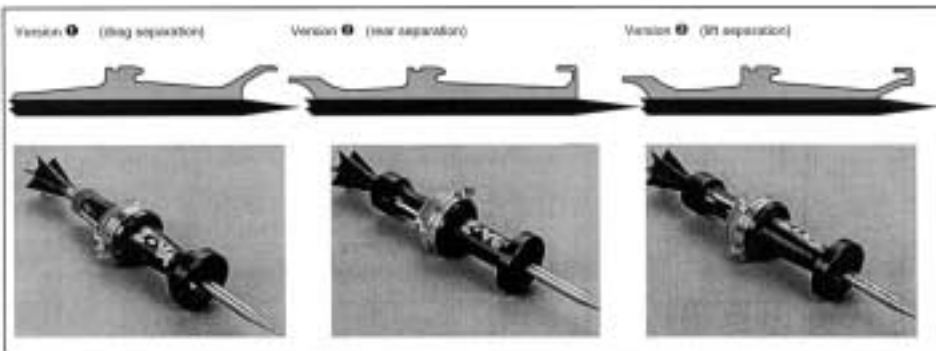


Fig. 3: Sabot shape versions.

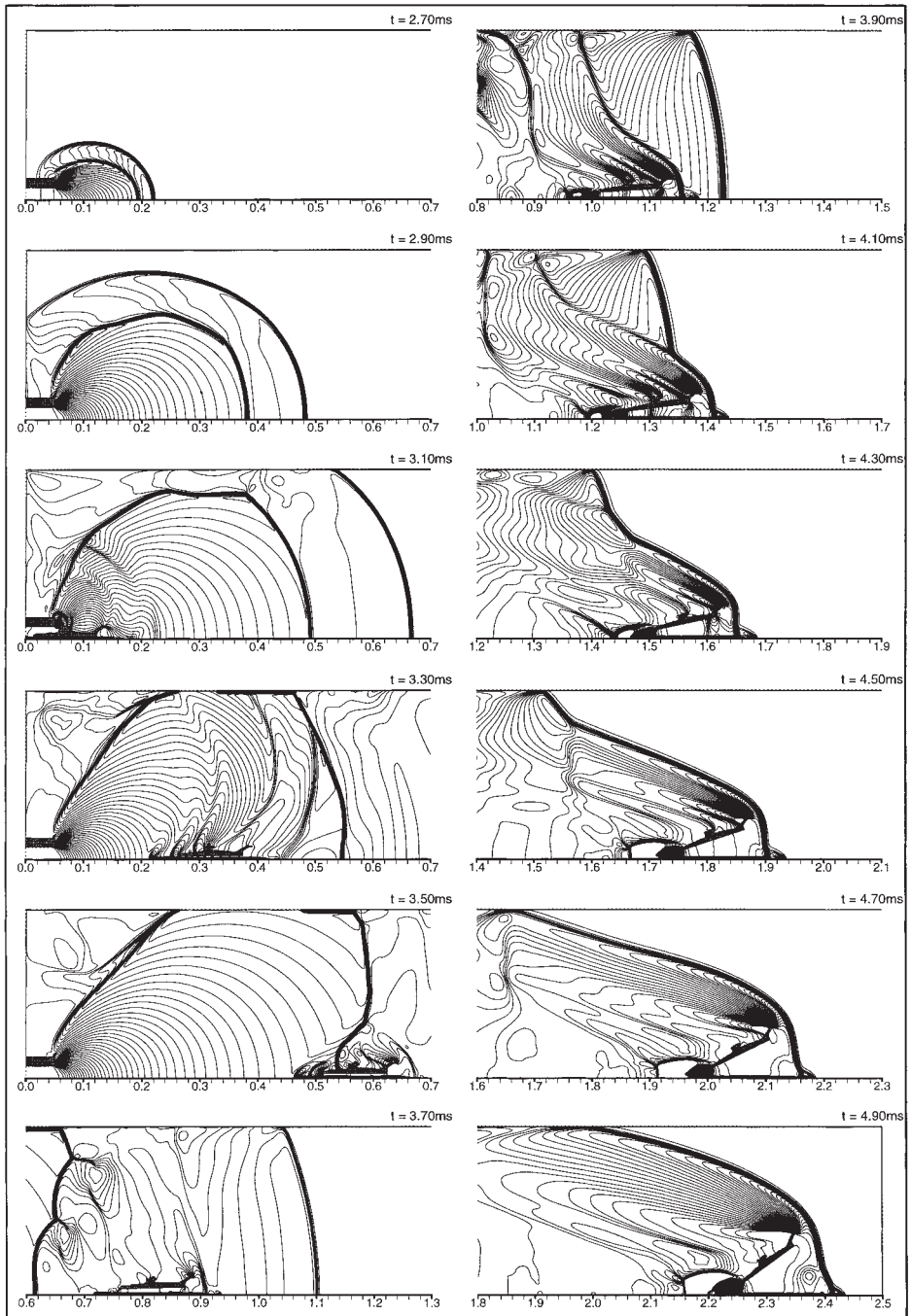


Fig 4: Computation of the time evolution of the drag separation process ( sabot version ① – grid 1500 x 180).



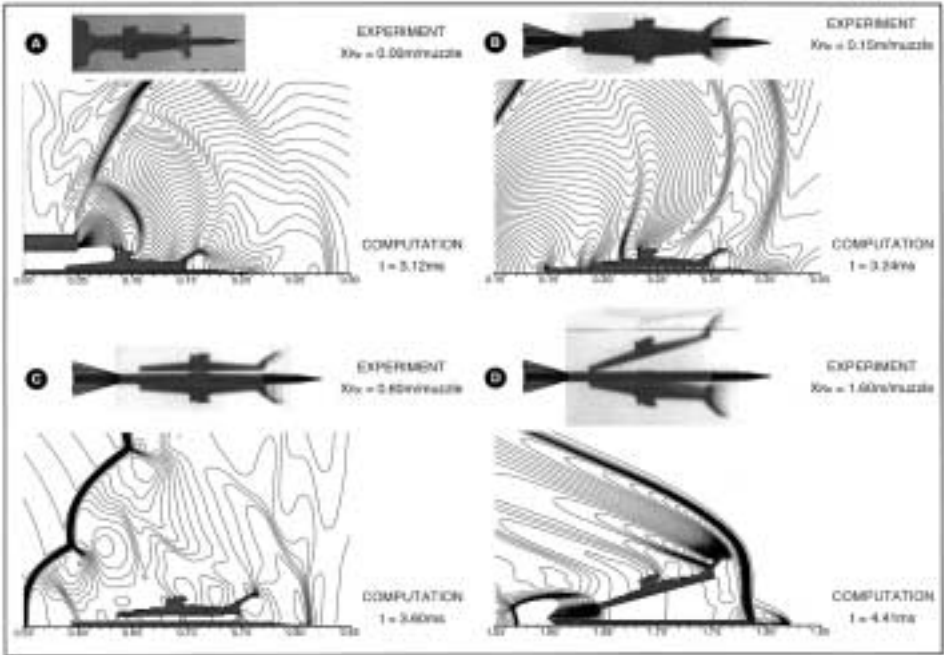


Fig. 5: Experimental and computational discard process comparison for sabot shape version ① (drag separation – grid 1500 x 180)

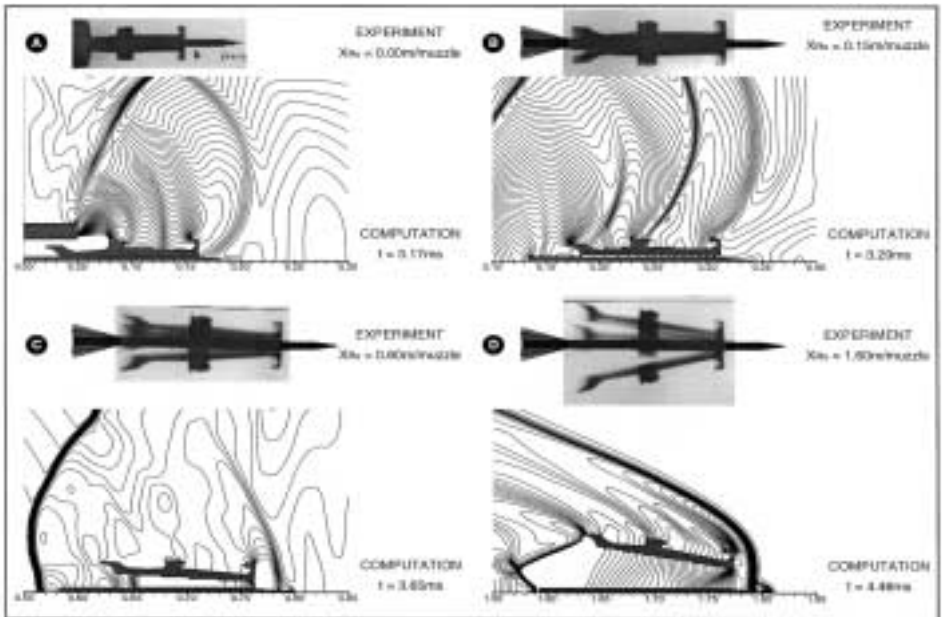


Fig. 6: Experimental and computational discard process comparison for sabot shape version ② (rear separation – grid 1500 x 180)



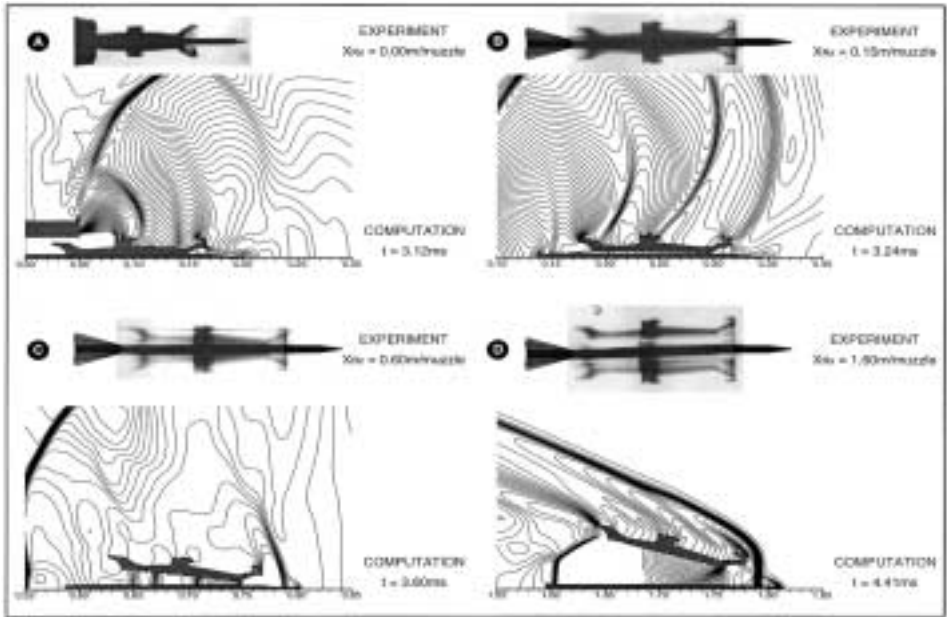


Fig. 7: Experimental and computational discard process comparison for sabot shape version ③ (lift separation – grid 1500 x 180)

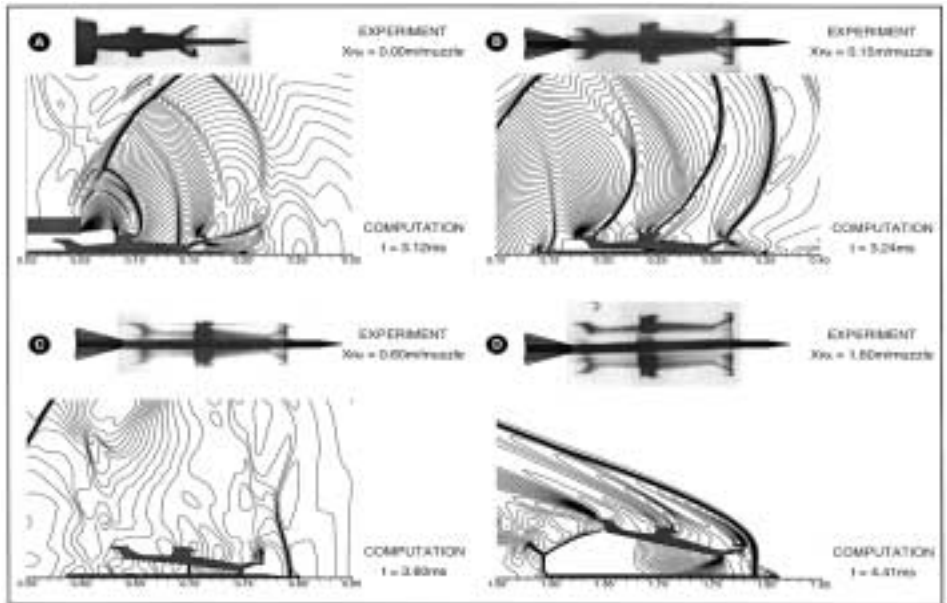


Fig. 8: Experimental and computational discard process comparison for sabot shape version ③ (rear separation – grid 3000 x 360)

